1986

An Experimental Study of a Single-Phase Natural Convection in a Cylindrical, Vertical Channel

S. Ali A. Hashemi
University of Central Florida

AN EXPERIMENTAL STUDY OF A SINGLE-PHASE NATURAL CONVECTION IN A CYLINDRICAL, VERTICAL CHANNEL

BY

S. ALI A. HASHEMI
B.S.E., University of Central Florida, 1982

RESEARCH REPORT

Submitted in partial fulfillment of the requirements
for the degree of Master of Science
in the Graduate Studies Program
of the College of Engineering
University of Central Florida
Orlando, Florida

Summer Term
1986

ABSTRACT

Presented in this paper is the first known experimental assessment of a single-phase natural convection in a cylindrical, vertical channel subjected to non-uniform or uniform heat flux. This work was conducted at the University of Central Florida in the College of Engineering.

The results of this experimental study were compared with theory. The experimental values of Nusselt numbers ($Nu = hD/K$) in the entrance and fully-developed regions were somewhat lower and higher, respectively, when compared with theory.

ACKNOWLEDGEMENTS

The author with gratitude to Dr. Fred Gunnerson for his encouragement, advice and support during all phases of his graduate study.

The author would also like to express his appreciations to Drs. Burton Eno, and E.R. Hosler in reviewing this report.

Thanks are also extended to the Department of Mechanical Engineering and the College of Engineering for the financial support provided during his graduate studies.

The author would also like to thank the faculty, staff, and graduate students of the Mechanical Engineering, specially Dr. Pasamehmetoglu, and Mr. Joshi.

The author wishes to extend special thanks to his parents, Ebrahim and Mehri Hashemi, and his brother and sister, for their inspiration and ever-lasting support during various phases of the author's education.

TABLE OF CONTENTS

LIST OF TABLES

LIST OF FIGURES

NOMENCLATURE

A	Area, m^2
A_s	Surface area, m^2
b	width of the channel, m
C_p	Specific heat at constant pressure, J/Kg-K
D	Diameter of the tube, m
f	temperature difference, $T-T_o$, K
F	Dimensionless volumetric flow rate
Gr	Grashof number, $g\,\beta(T_s-T_m)\,D^3/\,\nu^2$
Gr^*	Modified Grashof number, $g\beta\dot{q}_w R^3/\,K\nu^2$
Gr_I^*	Modified Grashof number, $g(\bar{T}_1-\bar{T}_o)r_\omega^4/\bar{T}_o L\nu^2$
Gr_{II}^*	Modified Grashof number, $gq''\,r_\omega^5/\bar{T}_o L\nu^2 K$
g	Gravitational acceleration, m/s^2
h	Convection heat transfer coefficient, W/m^2-K
i	Electric current density, A/m
H	Vertical height of heat transfer region, m
K	Thermal conductivity of the fluid, W/m-K
K_{ins}	Thermal conductivity of the insulation, W/m-K
K_1	Integration constant, Ref[2]
K_2	Integration constant, Ref[2]
L	Characteristic length, m
L'	Dimensionless tube length, $1/Gr_{II}^*$
$\dot{m}$	Mass flow rate, Kg/s

Nu_D	Nusselt number, hD/K
Nu_R	Nusselt number, hR/K
Nu_L	Nusselt number, hL/K
Nu_I	Nusselt number, Ref[11]
P	Perimeter, m
p	Pressure, N/m^2
Pr	Prandtl, ν/α
q	Heat transfer rate, W
q	Rate of energy generation per unit volume, W/m^3
q'	Heat transfer rate per unit length, W/m
q''	Heat flux, W/m^2
Q	Dimensionless heat dissipation rate, Ref[1]
r	Normalized radial coordinate
R	Cylinder radius, m
Ra	Rayleigh number, GrPr
Ra_I	Rayleigh number, $g\beta qb^5/L\nu\alpha K$
Ra_L	Rayleigh number, $g\beta(T_s-T_\infty)L^3/\nu\alpha$
Ra_D	Rayleigh number, $g\beta(T_s-T_\infty)D^3/\nu\alpha$
Ra'	First modified Rayleigh number, $\rho^2 C_p g\beta b^4(T_w-T_o)/\mu KH$
Ra''	Second modified Rayleigh number, $\rho^2 C_p g\beta b^5 q''/\mu K^2 H$
Re	Reynolds number, $4\dot{m}/\pi D\mu$
R	Electric resistance, Ohms
T	Temperature, K

T_1	Temperature of wall, K
T_o	Ambient temperature, K
$\overline{T}_o$	Absolute ambient temperature, K
T_s	Surface temperature, K
t	time, s
u,v	Mass average fluid velocity components, m/s
V	Fluid velocity, m/s
x,y	Rectangular coordinates, m

GREEK LETTERS

α	Thermal diffusivity, m^2/s
β	Volumetric thermal expansion coefficient, 1/K
μ	Viscosity, Kg/m-s
ν	Kinematic viscosity, m^2/s
ρ	Mass density, Kg/m^3
υ	Specific volume, m^3/Kg

SUBSCRIPTS

R	Radius taken at characteristic length
o	Centerline conditions
w	Wall conditions
b	Bulk conditions
s	Surface conditions

1. INTRODUCTION

Natural convection heat transfer and the resulting mass flow within a vertical channel subjected to a constant uniform heat flux is of fundamental interest within the technical community. Such conditions may be found within a variety of thermal equipment including commercial nuclear reactors, solar and electronic components.

Stringent licensing procedures for commercial nuclear reactor operation require detailed investigations of the phenomena associated with normal and postulated accident situations. The result of many postulated accident scenarios is the sole dependence on natural or free convective core cooling. Unfortunately, exact analytical modeling of free convection behavior within a reactor geometry is complicated by flow disruptions due to spacers, non-uniform axial heat addition, gamma heating, generation of two-phase flow and a host of other considerations. Therefore efforts must focus on simplified analytical treatments or on empirical approaches, which are often limited in application and may mask the physics.

The analysis of a solar thermal chimney design also requires natural convection analysis. Such a chimney serves

as an outlet and circulation aid for the air of a dwelling and is powered by the incident solar flux.

The cooling of electronic equipment by natural convection is common. While in service, the geometry may be such that natural convection in a vertical channel with high length to diameter ratio may be neccesary.

The theoretical analysis covering the general aspects of the above problem have been presented in Reference [1], the first known analytical assessment of natural convection in a vertical channel with uniform heat flux. The flow is assumed to be stable and laminar. The incompressible thermal boundary layer equations for this situation were solved by a finite difference method.

The other theoretical analysis of the above problem has been presented in Reference [2]. The solution assumes that the flow is through a vertical circular channel, the heat flux is uniform in the axial and peripheral directions, and the natural convection flow is laminar, incompressible, fully developed and one-dimensional.

The basic governing equations (continuity, momentum, and energy) are combined into a fourth order ordinary differential equation and infinite series solution of the resulting equation is obtained. The results provide temperature and velocity profiles for the flow, mass flow

rate, and also indicate that the Nusselt number reaches a constant value as in the case of forced convection.

Chapter 2 presents the basic concepts of natural convection heat transfer and introduces the governing equations. Also included is a brief survey of internal flow for different geometries and boundary conditions. The experimental setup, test techniques and data measurements methods are detailed within Chapter 3.

The experimental test section used in the present investigation is detailed in Chapter 3. It consists of an adjustable copper tube with a total length of 975 mm, outside diameter of 16.3 mm, and inside diameter of 14.3 mm. The test section is held vertically. To evaluate the theoretical analysis, and the associated assumptions, an experimental test program was designed. A portable, twelve-centimeter long copper test section with uniform heat flux and instrumented with five thermocouples equally spaced along its length was installed. The total length of the channel is adjustable and air is the working fluid. From the utility point of view, the instrumented test section can be placed anywhere along the channel.

The results of the theoretical and experimental investigations are presented in this report. The surface temperature and the heat transfer data, as well as a discussion about the possibility of obtaining laminar fully

developed natural convection flow are also included in this report. The possibility of obtaining a correlation for the Nusselt number is discussed.

Chapter 3 also presents the results and compares theory with experiment. The conclusion of this study, along with some final closing remarks, is given in Chapter 4.

2. THEORETICAL CONSIDERATIONS

2.1 General Remarks

One important task of an engineer is to calculate the energy transfer rates across a solid-fluid interface where the fluid is moving relative to the solid. When there is fluid motion, energy is transported by the movement of the fluid. This process is called convection. This mode of heat transfer is comprised of two mechanisms, one which is the random molecular-motion (diffusion), and the other is that energy is transferred by the bulk, or macroscopic, motion of the fluid.

If the fluid motion involved in a process is induced by some external means (pump, blower, vehicle motion, wind, etc.) the process is called forced convection. For free (natural) convection the flow is induced by buoyancy forces in the fluid which are due to the presence of density gradient within the fluid and a body force that is proportional to the fluid density. The body force is usually gravitational, although it may also be due to centrifugal force or Coriolis force.

Consider fluid flow over the heated surface as illustrated in Figure (2.1). The viscous fluid-solid interaction develops a boundary region in which the velocity varies from zero at the surface to a finite value U associated with the distant flow. This region of the fluid is called the hydrodynamic or velocity boundary layer. In reality there is no precise thickness to the boundary layer and its thickness is generally defined as the distance in which 99% of the velocity change takes place.

Consider steady flow along the surface shown in Figure (2.2) with a free stream velocity U_∞, and a free stream temperature T_∞. If the surface temperature T_S and the fluid temperature T_∞ differ, there will be a region of the fluid over which the temperature varies from T_S at y=0 to T_∞ in the outer flow. This region is called the thermal boundary layer. Depending on the Prandtl number of the flow, the thermal boundary layer may be smaller, larger, or the same thickness as the velocity boundary layer. If T_S is greater than T_∞, convection heat transfer will occur from the surface to the outer flow.

The description of the convective heat transfer mode is rooted in the energy transfer occurring within a fluid. For single-phase convection, the energy transferred contributes to the sensible (internal thermal) heat of the fluid. There are two-phase convective processes where the latent heat

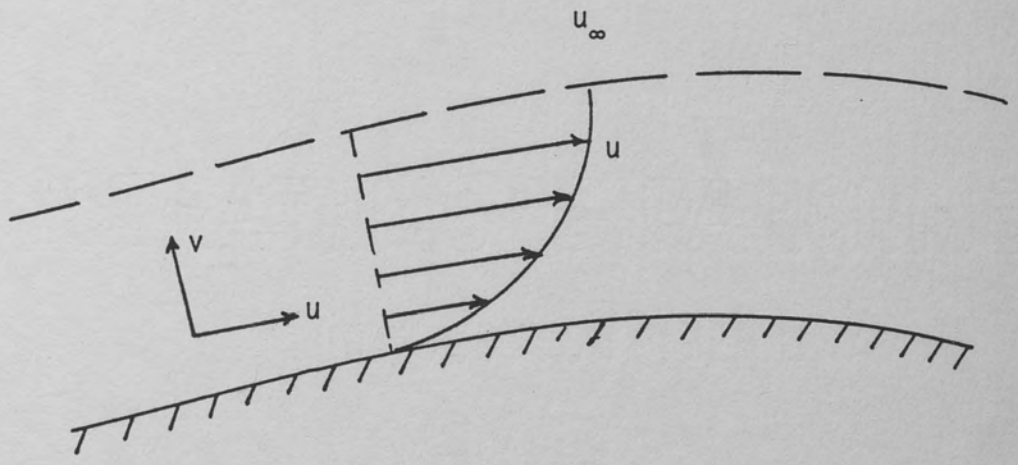

Figure 2.1. Velocity boundary layer.

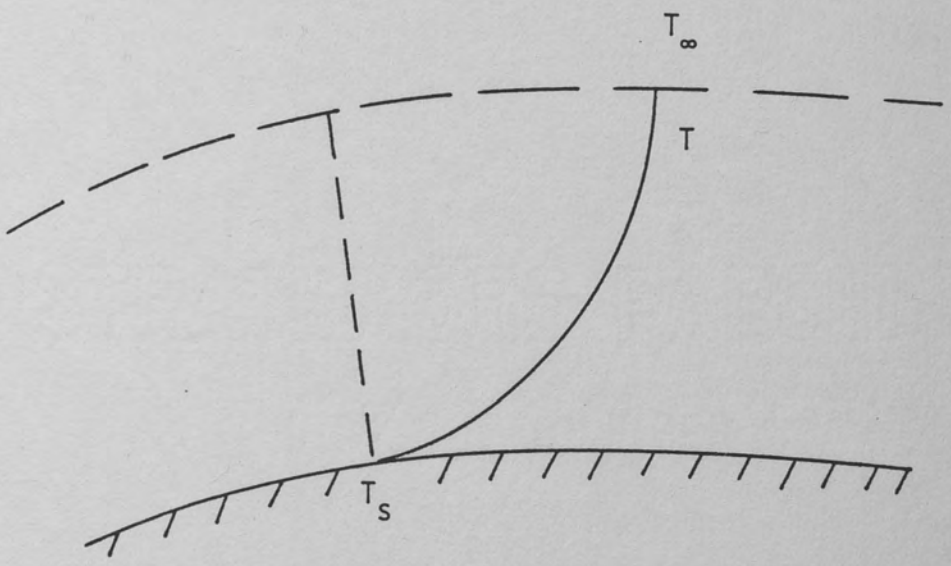

Figure 2.2. Thermal boundary layer.

must be considered when boiling or condensation occurs. The latent heat of vaporization is associated with a phase change between the liquid and vapor states of the fluid.

Regardless of the nature of the convective heat transfer process, the appropriate rate equation is generally of the form:

$$q'' = h (T_s - T_\infty) \qquad (2.1)$$

where the convective heat flux $q''(W/m^2)$ is proportional to the difference between the surface temperature and the fluid temperature. This expression is known as Newton's Law of Cooling, and the proportionality constant, h $(W/m^2 -K)$, is referred to as the convective heat transfer coefficient, the film conductance, or the film-coefficient. The heat transfer coefficient depends on the following:

(i) The conditions in the boundary layer, which depend, in part, on the surface geometry,

(ii) The nature of the fluid motion, and

(iii) A number of the fluid thermodynamic and transport properties.

Ultimately, any study of thermal convection reduces to a study of how the heat transfer coefficient may be determined.

The approximate ranges of convective heat transfer coefficients are indicated in Table (2.1).

TABLE 2.1

APPROXIMATE VALUES OF CONVECTION HEAT TRANSFER COEFFICIENT

Mode	Heat Transfer Coefficient $h(W/m^2-k)$
Free Convection	5-25
Forced Convection	
Gases	25-250
Liquids	50-20,000
Convection with Phase Change Boiling or Condensation	2500-100,000

Reference [3]

2.2. Free-Convection Heat Transfer on a Vertical Flat Plate

Consider the vertical flat plate shown in Figure 2.3. This is perhaps the simplest case in natural convection. When the plate is heated, a free-convection boundary layer is formed and driven by buoyancy forces. These forces are modeled by the momentum equation. To analyze the heat transfer problem, one must first obtain the differential equation of motion for the boundary layer. The assumptions generally considered are:

(i) constant thermal properties

(ii) incompressible

(iii) steady state

(iv) two-dimensional conditions in which the gravity force acts in the negative x-direction.

With these assumptions, the x-momentum equation is

$$u(\partial u/\partial x)+v(\partial u/\partial y)= -1/\rho(\partial p/\partial x)-g+\nu(\partial^2 u/\partial y^2) \qquad (2.2)$$

and the pressure gradient in the x-direction is;

$$(\partial p/\partial x)= -\rho_\infty g \qquad (2.3)$$

Substituting Equation (2.3) into Equation (2.2),the following relationship is obtained;

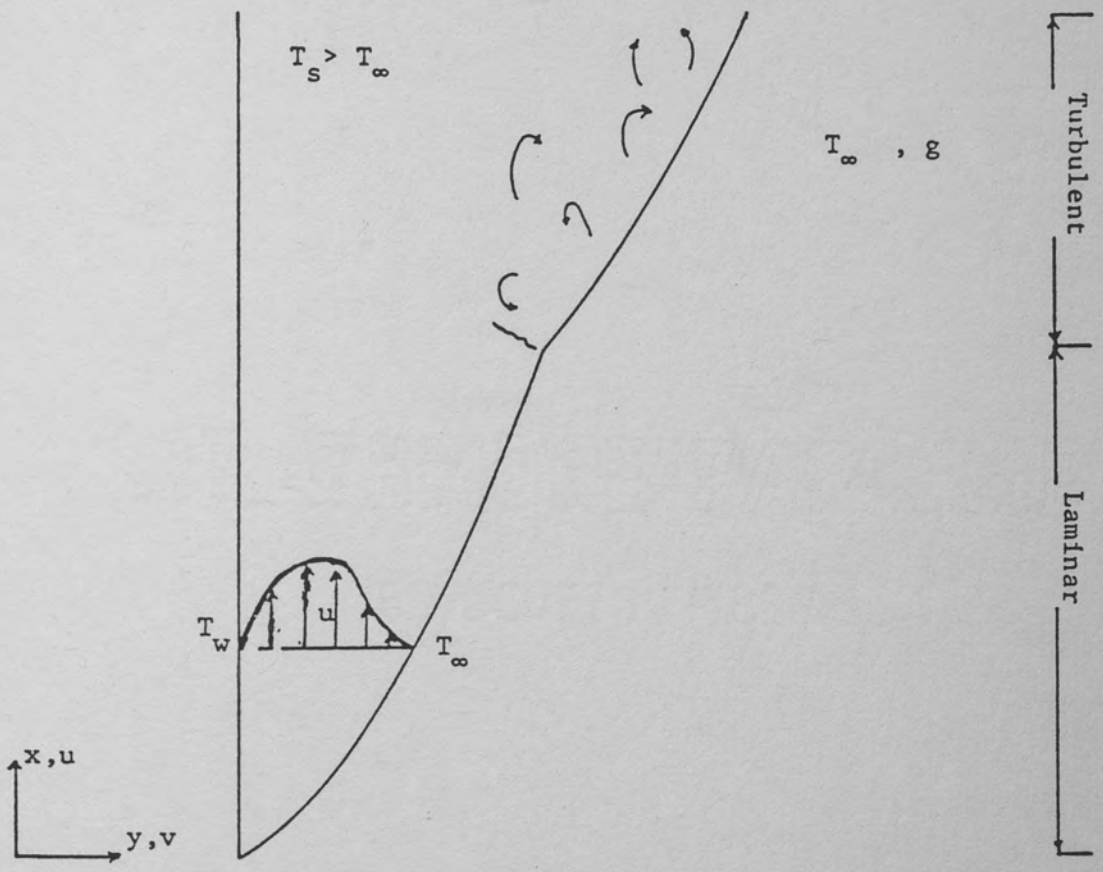

Figure 2.3. Thermal boundary layer for a flat plate.

$$u(\partial u/\partial x)+v(\partial u/\partial y) = (g/\rho)(\rho_\infty-\rho)+\nu(\partial^2 u/\partial y^2) \qquad (2.4)$$

The first term on the right hand side of Equation (2.4) corresponds to the buoyancy force from which the flow originates. The volumetric thermal expansion coefficient is defined by;

$$\beta = (-1/\rho)(\partial\rho/\partial T)_p \qquad (2.5)$$

which can be expressed in the following approximate form;

$$\beta = (-1/\rho)[(\rho_\infty-\rho)/(T_\infty-T)] \qquad (2.6)$$

Substituting Equation (2.6) into Equation (2.4), the x-momentum equation becomes;

$$u(\partial u/\partial x)+v(\partial u/\partial y) = g\ \beta(T-T_\infty)+\nu(\partial^2 u/\partial y^2) \qquad (2.7)$$

Equation (2.7) relates the buoyancy force to the temperature difference.

The continuity equation and the energy equation remain the same as for the forced convection with the exception that the viscous dissipation is neglected in the energy equation, which is a reasonable assumption for low velocities associated with free convection. The set of governing equations is then as follows:

$$(\partial u/\partial x)+(\partial v/\partial y) = 0 \tag{2.8}$$

$$u(\partial u/\partial x)+v(\partial u/\partial y) = g(T- T_{\infty})+\nu(\partial^2 u/\partial y^2) \tag{2.9}$$

$$u(\partial T/\partial x)=v(\partial T/\partial y) = \alpha(\partial^2 T/\partial y^2) \tag{2.10}$$

More in-depth presentation of the continuity, momentum, and energy equations can be found in Reference[3].

Nondimensionalizing the governing equations is done by using the following parameters:

$$x^* \equiv x/L \quad y^* \equiv y/L$$
$$u^* \equiv u/u_0 \quad v^* \equiv v/u_0 \quad T^* \equiv (T-T_{\infty})/(T_s-T_{\infty}) \tag{2.11}$$

The x-momentum and energy equations, Equations (2.9) and (2.10), respectively, reduce to,

$$u^*(\partial u^*/\partial x^*)+v^*(\partial u^*/\partial y^*)= \frac{g\beta(T_s-T_\infty)L}{u_o^2}\, T^*+(1/Re_L)(\partial^2 u^*/\partial y^{*2}) \qquad (2.12)$$

$$u^*(\partial T^*/\partial x^*)+v^*(\partial T^*/\partial y^*)= (1/Re_L Pr)(\partial^2 T^*/\partial y^{*2}) \qquad (2.13)$$

The first dimensionless parameter which appears in the right hand side of equation (2.12) is because of the buoyancy force. It is in terms of the unknown reference velocity u_o, and it can be presented in terms of a Grashof number as follows:

$$Gr_L= \frac{g\beta(T_s-T_\infty)L}{u_o^2}\,(u_o L/\nu)^2= [g\beta(T_s-T_\infty)L^3]/\nu^2 \qquad (2.14)$$

The role of the Grashof number (the ratio of buoyancy force relative to the viscous force acting on the fluid) in free convection is analogous to the role of the Reynolds number (the ratio of inertial to viscous forces acting on a fluid element) in forced convection.

The dimensionless group (Gr/Re^2) is a measure of the ratio of buoyancy forces to inertial forces in the flow. Generally, the following free/forced convection criteria are applicable:

$(Gr/Re^2) \gg 1$	"Pure" free convection
$(Gr/Re^2) \cong 1$	Mixed convection
$(Gr/Re^2) \ll 1$	"Pure" forced convection

The governing equations related to the current research are disscussed in Section 2.4, where difficulties associated in solving these equations are also pointed out.

2.3 Empirical Correlations For Internal Flow

As illustrated in Figure 2.4, the use of free convection heat transfer from the vertical parallel plate channel is made. Similar techniques are utilized in the cooling of electronic equipment, the transfer of process heat in the chemical industry, and the dissipation of condenser heat from air conditioning and refrigeration equipment.

The local heat transfer coefficient for the vertical, parallel plate channel is dependent on both the height of the plates, and their distance of separation. Table 2.3. summarizes the Nusselt number relations for short and tall, parallel plate channels for various boundary conditions.

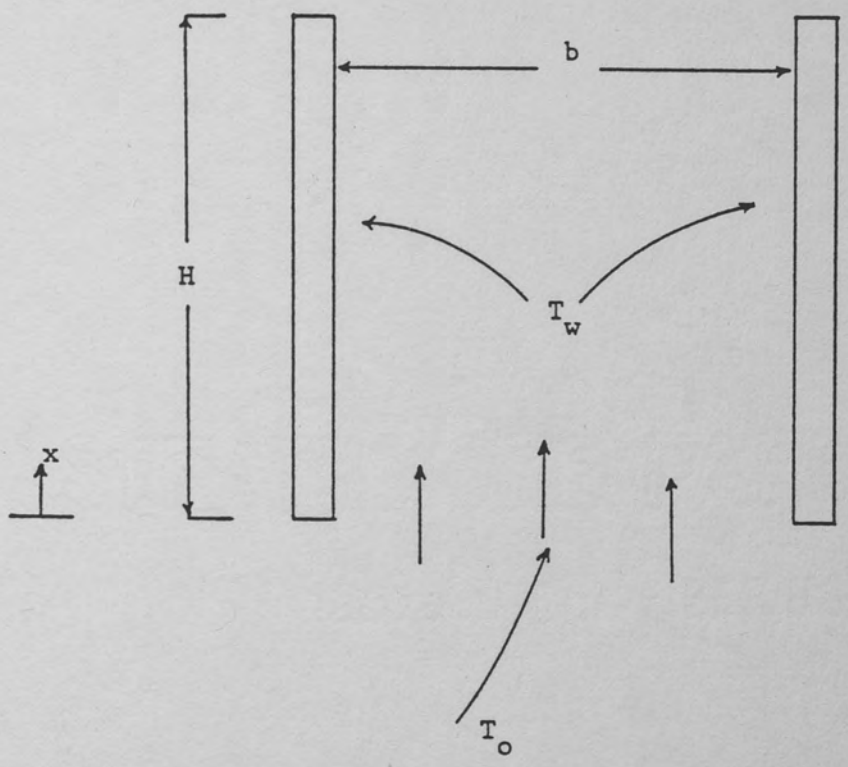

Figure 2.4. Schematic of flow in vertical channel.

TABLE 2.2
SUMMARY OR FREE CONVECTION RELATIONS FOR VERTICAL PARALLEL PLATE GEOMETRIES. LAMINAR FLOW.

Boundary Condition	Restriction(s)	Relation	References
Symmetrically Isothermal Channel	Small H/b	2.15	4
	Large H/b	2.16	5, 6, 7
Asymetrically Isothermal channel	$\frac{T_2 - T_o}{T_1 - T_o} = 1.0$	2.16	7
	$\frac{T_2 - T_o}{T_1 - T_o} = 0.5$	2.17	7
	$\frac{T_2 - T_o}{T_1 - T_o} = 0.1$	2.18	7
	$\frac{T_2 - T_o}{T_1 - T_o} = 0.0$	2.19	7
	one wall Insulated & large H/b	2.20	8
Symmetrically Isoflux Channel	Small H/b	2.21	9
	Based on midheight temperature	2.22	9
	Large H/b	2.23	7
	Based on midheight temperature	2.24	
Asymmetrically Isoflux Channel	Large H/b	2.25	10
	Based on midheight temperature	2.26	10

$$Nu_o = 0.53 \left(Ra' \right)^{1/4} \tag{2.15}$$

$$Nu_o = 1/24 \left(Ra' \right) \tag{2.16}$$

$$Nu_o = 17/405 \left(Ra' \right) \tag{2.17}$$

$$Nu_o = 79/1815 \left(Ra' \right) \tag{2.18}$$

$$Nu_o = 2/45 \left(Ra' \right) \tag{2.19}$$

$$Nu_o = 1/12 \left(Ra' \right) \tag{2.20}$$

$$Nu_o = 0.519 \left(Ra'' \right)^{1/5} \tag{2.21}$$

$$Nu_o = \left(Ra''/48 \right)^{1/2} \tag{2.22}$$

$$Nu_o = \left(Ra''/24 \right)^{1/2} \tag{2.23}$$

$$Nu_{o,H/2} = 0.73 \left(Ra'' \right)^{1/5} \tag{2.24}$$

$$Nu_{o,H/2} = \left(Ra''/12 \right)^{1/2} \tag{2.25}$$

$$Nu_{o,H/2} = \left(Ra''/6 \right)^{1/2} \tag{2.26}$$

$$Ra' = \rho^2 C_p g \beta b^4 (T_w - T_o)/\mu K H$$

$$Ra'' = \rho^2 C_p g \beta b^5 q''/\mu K^2 H$$

Wirtz and Stutzman [11] conducted experimenmts on free convection between vertical plates with uniform heat flux, where the working fluid was air. From their results, a design equation was found which predicts the local Nusselt number at the top of the plate:

$$Nu_I(L) = 0.144\ Ra_L^{\frac{1}{2}} / (1+0.0156\ Ra_L^{0.9})^{0.33} \qquad (2.27)$$

$$[Nu_I(x)/Nu_I(L)] = [T_w(x)-T_o]/[T_w(L)-T_o] = (x/L)^m \qquad (2.28)$$

The temperature variation of the plate may be calculated from this information.

Wirtz and Stutzman [11] also provide information for predicting the local Nusselt number and plate temperature variation. Combining equations (2.27) and (2.28), as shown in Figure 2.5, the local Nusselt number can now be calculated.

The results obtained by Wirtz and Stutzman are in close agreement with the finite difference calculations of Aung, Fletcher and Sernas [12].

Elenbaas [5] considered the transfer of heat by free convective flow of a gas in heated, open vertical tubes of

different shapes and cross-sections. He carried out extensive analytical and experimental work on natural convective flow in such cross-sectional geometries as the equilateral triangle, square, rectangle, circle, and infinite parallel plates. Elenbaas obtained an approximate solution for a uniform wall temperature and assuming that the radial velocity component v was zero. His analytical solution is

$$Nu_{r,w} = (1/16)\ Gr^{*}_{w}\ Pr[1-\exp(-1/16\ (5/Gr^{*}Pr)^{3/4})] \qquad (2.29)$$

He concluded (from his experimental observation) that equation (2.29) holds within about 10% for all shapes of cross-sections.

Much of the previous published work on natural convection was shown in the previous pages. For natural convection in a vertical circular tube with uniform heat flux, Davis and Perona [1] solved the problem by the finite difference method and compared the results with those of Kays [13] on laminar forced convection which is presented in Figure C.2 in Appendix C. The work, which is presented in the following sections, is a simple experiment on natural convection in a vertical tube with uniform heat flux. A comparison between the experiment and the work of Davis and Perona is also provided.

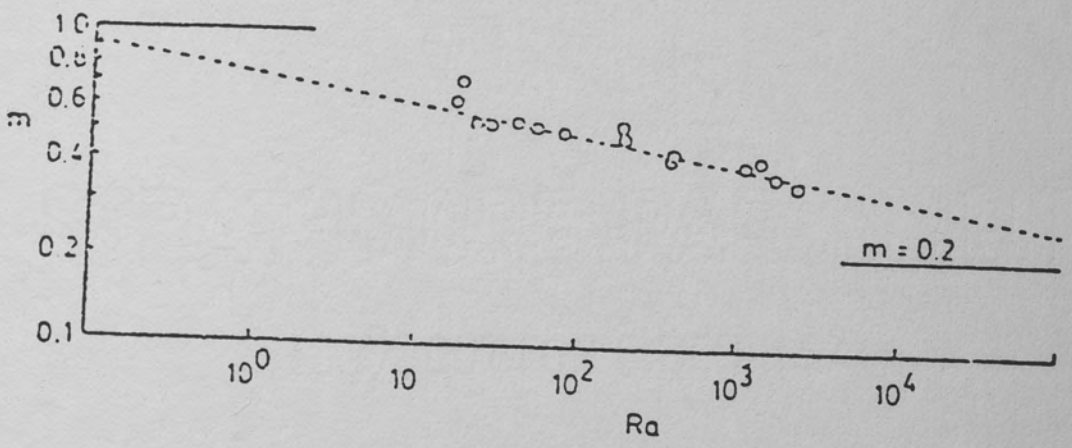

Figure 2.5. Experimentally determined values of the exponent "m" of equation (2.28) Reference [1].

2.4 Governing Equations and Solution Technique

The basic governing equations (continuity, momentum and energy) in radial coordinates are given by the expressions:

$$(v/r)+(\partial v/\partial r)+(\partial u/\partial x) = 0 \qquad (2.30)$$

$$v(\partial u/\partial r)+u(\partial u/\partial x)= \nu[(\partial^2 u/\partial r^2)+(1/r)(\partial u/\partial r)]-(1/\rho)(\partial p/\partial x)-g \qquad (2.31)$$

$$v(\partial T/\partial r)+u(\partial T/\partial x)= \alpha[(\partial^2 T/\partial r^2)+(1/r)(\partial T/\partial r)] \qquad (2.32)$$

As can be seen, the above equations are non-linear partial differential equations. They require complex mathematical methodology for analytical solution, and consumes excessive computational time for solving numerically. Davis and Perona [1] have provided the velocity and temperature distributions throughout the tube by solving the thermal boundary layer equations in dimensionless form by a finite difference technique. Their solutions for the cases of constant wall temperature and constant wall heat flux are presented in the following pages (Figures 2.6, 2.7, 2.8, and 2.9).

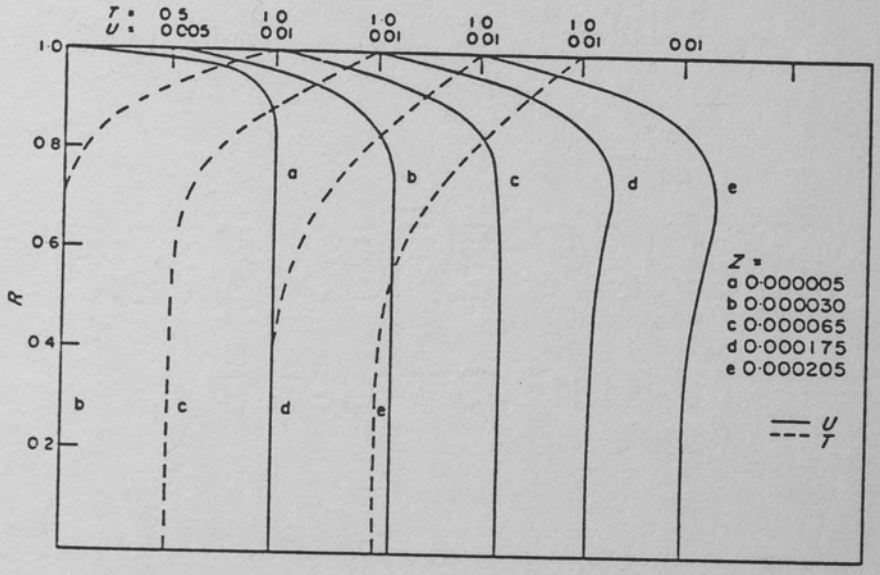

Figure 2.6. Velocity and temperature profile for Q=0.0095, constant wall temperature, large D, Reference [1]

$$Q = q/(\pi \rho C_p L \nu Gr^*(T_L - T_o))$$

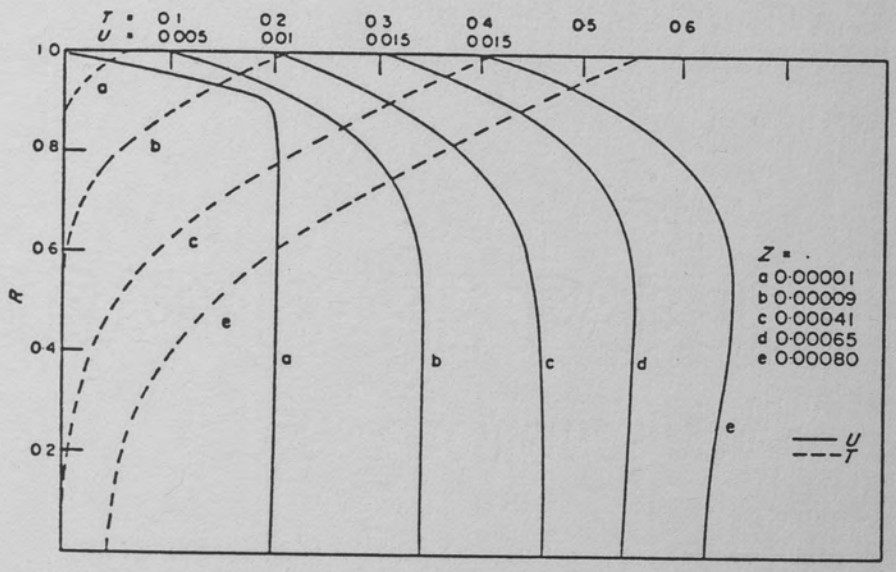

Figure 2.7. Velocity and temperature profile for Q=0.0096, constant heat flux, large D, Reference [1].

$Q = 2z/(Pr\ Gr^{*}\ L)$

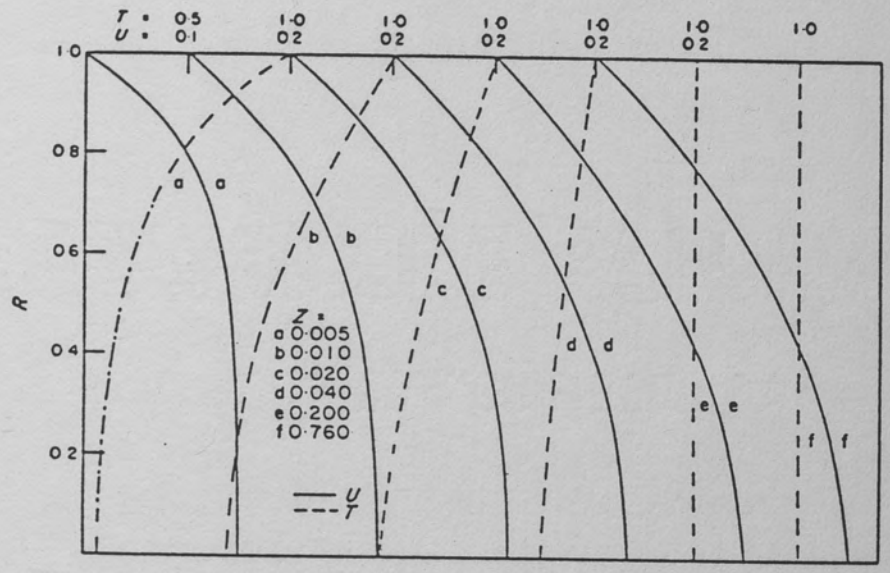

Figure 2.8. Velocity and temperature profile for Q=0.12, constant wall temperature, small D, Reference [1].

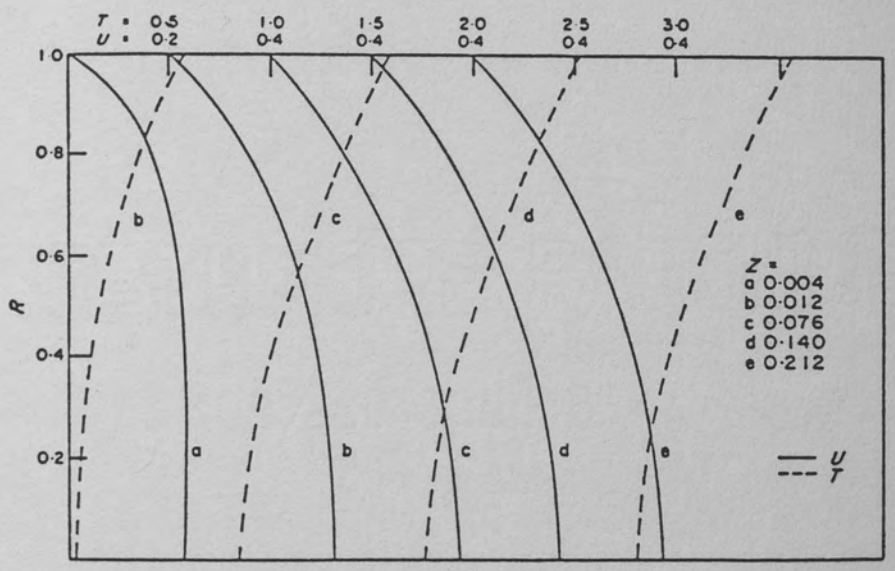

Figure 2.9. Velocity and temperature profile for Q=0.193, constant heat flux, small D, Reference [1].

Pasamehmetoglu [2] also provides an analytical solution of fully developed natural convection in a vertical channel with uniform heat flux. His solution assumes that the flow is through a vertical circular channel, the heat flux is uniform in the axial and peripheral directions, and the natural convection flow is laminar, incompressible, fully developed, and one dimensional. The basic governing equations (continuity, momentum and energy) with the above assumptions are :

$$(\partial u/\partial x)=0 \tag{2.33}$$

$$\nu[(1/r)\partial/\partial r(r\partial u/\partial r)]+g\beta(T-T_0)=0 \tag{2.34}$$

$$\alpha[(1/r)\partial/\partial r(r\partial T/\partial r)]-u(\partial T/\partial x)=0 \tag{2.35}$$

His solution is provided in Appendix A. The results provide temperature and velocity profiles for the flow, mass flow rate, and also indicate that the Nusselt number reaches a constant value as in the case of forced convection.

Due to the inherent difficulty in solving the above simultaneous equations mathematically, the information leading to velocity and temperature profiles by the experimental means is necessary.

The method of solution generally in a forced convection problem is that the velocity profile is found first, and then it is used to derive the temperature profile. However, for the case of natural convection the velocity and temperature profiles are related and determined together. Also, the differential equations which are listed on the previous pages, contain non-linear terms and cannot be solved in closed form. To solve these equations one has to linearize the equations or solve the non-linear differential equations numerically.

The objective of most studies in a convection problem is to determine the heat transfer rate. The temperature distrubution can be used along with Newton's Law of Cooling to estimate the heat transfer rate.

3. EXPERIMENT

Within the following sections the experimental setup, test technique and data measurement techniques are presented.

3.1 Experimental Set up

A schematic view of the test section is shown in Figure 3.1. It consists of an adjustable copper tube with a length of 975mm, outside diameter of 16.3 mm, and inside diameter of 14.3 mm. The test section is held vertically. From the utility point of view, a 120 mm long instrumented test section is included. This instrumented portion of the test section contains five thermocouples (T-Type), equally spaced along it's length. In order to heat the entire vertical test section, an insulated copper wire (AWG of size 20) was uniformly wrapped (without any gap) along the total heated length. A conventional (0-30 volts, 0-25 amperes) power supply was used to provide a direct current (dc) to the copper wire for the resistance or joule heating.

The analog thermocouple outputs from the instrumented test section were recorded and digitized by a Digitec thermocouple thermometer. A foam-type pipe insulation (about

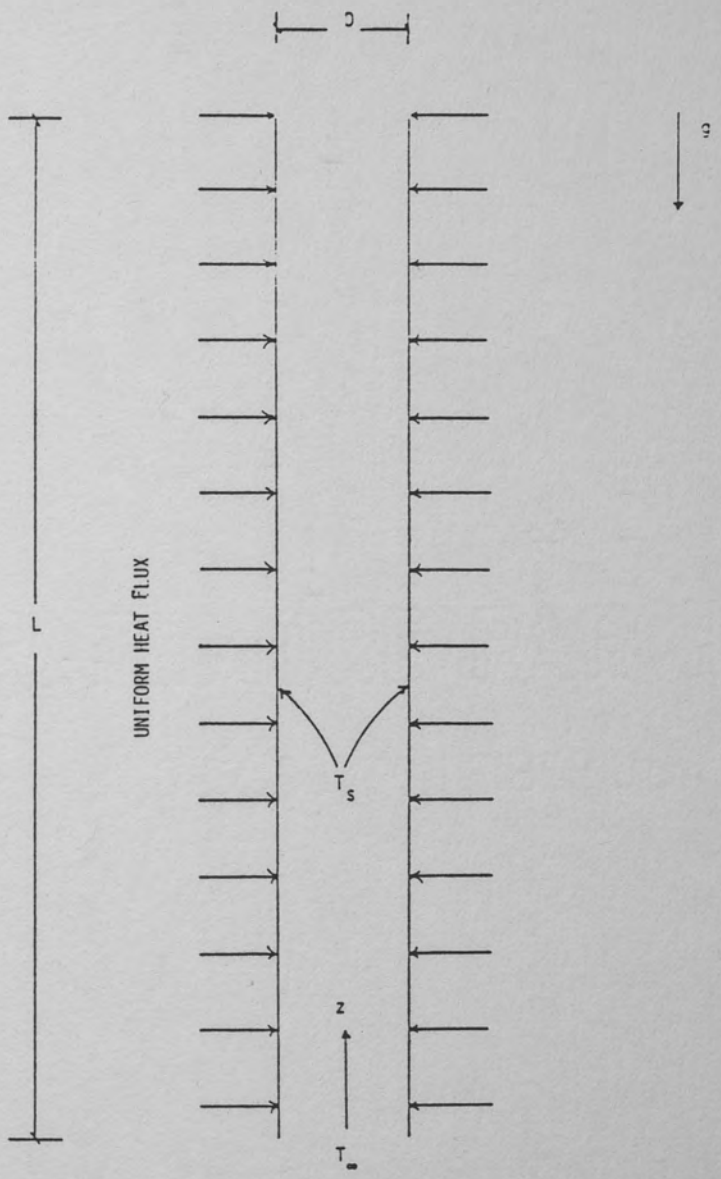

Figure 3.1 Schematic view of the test section.

1.6 centimeter thickness) was carefully wrapped around the heated test section to approximate a uniform heat flux along the length. As explained later, a nonuniform insulation thickness was necessary to better approximate a uniform heat flux. A conventional Psychrometer with air flow by a motor-driven fan was used to record the room conditions (temperature and humidity).

3.2 Test Technique

The entire 975 mm long heated section is divided into eight 120 mm long interconnectable subsections. One of the eight subsections is instrumented with five equally spaced thermocouples. The instrumented section can be moved from its original position to measure surface temperatures along the tube length. This flexible arrangement enables axial temperature measurements to be determined with minimal thermal instrumentation.

To maintain a uniform heat flux, energy analyses were carried out to evaluate the thermal insulation thickness required. The analysis used an external free convection mode around the insulation and required surface temperature data at various axial locations. The result indicated a non-uniform insulation thickness along the length was needed. These calculations are presented in Appendix B. The tests were conducted at a standard room temperature of 25 °C (dbt) and 20 °C (wbt).

3.3 Data And Measurement Techniques

Once the test section was prepared as shown in Figure 3.2 the data were measured as described below.

1) The necessary room conditions (temperature and humidity) were measured with a conventional psychrometer.

2) As shown in Figure 3.2, the instrumented section equipped with thermocouples was placed in the first measurement position.

3) The power supply and Digitec thermometer were turned on. The power supply was adjusted to give an initial heat flux of about 140 watts per square meter. The Digitec thermometer was also calibrated to measure the surface temperatures.

4) Sufficient time was allowed to establish a thermal equilibrium along the test section. Approximately 90 minutes of idle time was necessary between the initiation of power and the recording of temperatures.

5) Once the temperatures were measured at the initial position of the instrumented section, the power supply and the Digitec thermometer were disconnected in order to switch the insurmented section to its next axial position for the measurements. Steps 3 and 4 were repeated.

Figure 3.2 Photographs of the experimental setup.

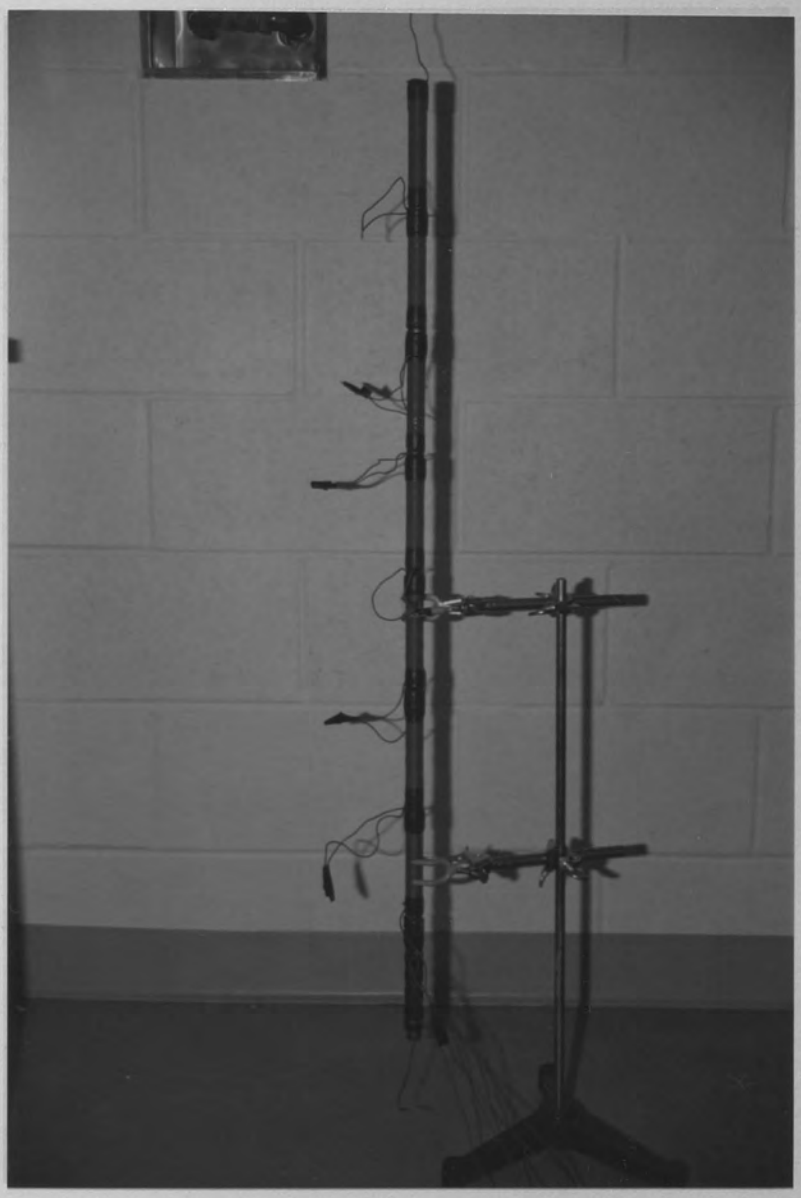

Figure 3.2 (Continued)

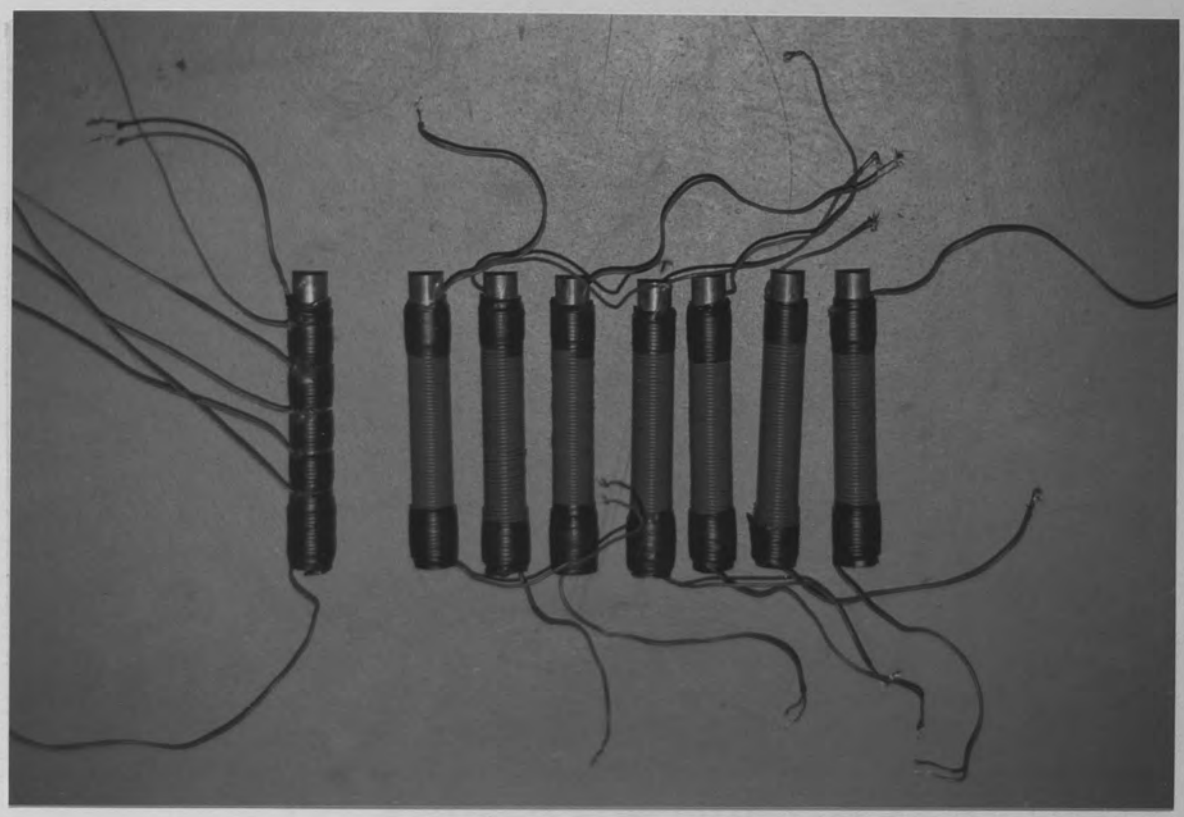

Figure 3.2 (Continued)

3.4 Experiment and Data Trend

The data obtained, for a uniform heat flux on a vertical tube, from this experiment are provided in this section. Typical axial surface temperatures for a constant heat flux of about 140 watts per square meter are illustrated in Table (3.1) and shown in Figure (3.3). The experimental and theoretical [1] Nusselt numbers are given in Table (3.2) and Figure (4.3), repectively. A brief disscusion is provided in the following section.

TABLE 3.1
THE AXIAL SURFACE TEMPERATURES ALONG THE TUBE.

x (cm)	T_S (°C)
3.5	37.2
5.5	37.4
9.5	38.5
15.5	40.5
17.5	40.6
21.5	41.0
27.5	41.4
29.5	41.3
33.5	42.4
39.5	43.5
41.5	44.1
45.5	44.2
51.5	46.1
53.5	45.9
57.5	46.6
63.5	48.3
65.5	48.4
69.5	48.7
75.5	49.6
77.5	49.8
81.5	50.1
87.5	51.2
89.5	51.1
93.5	51.8

T_S = 25 ± 1.0 °C
$D_=$ = 14.3 mm
q = 141 Watts per square meter
L = 975 mm
T_{out} = 42.9 C

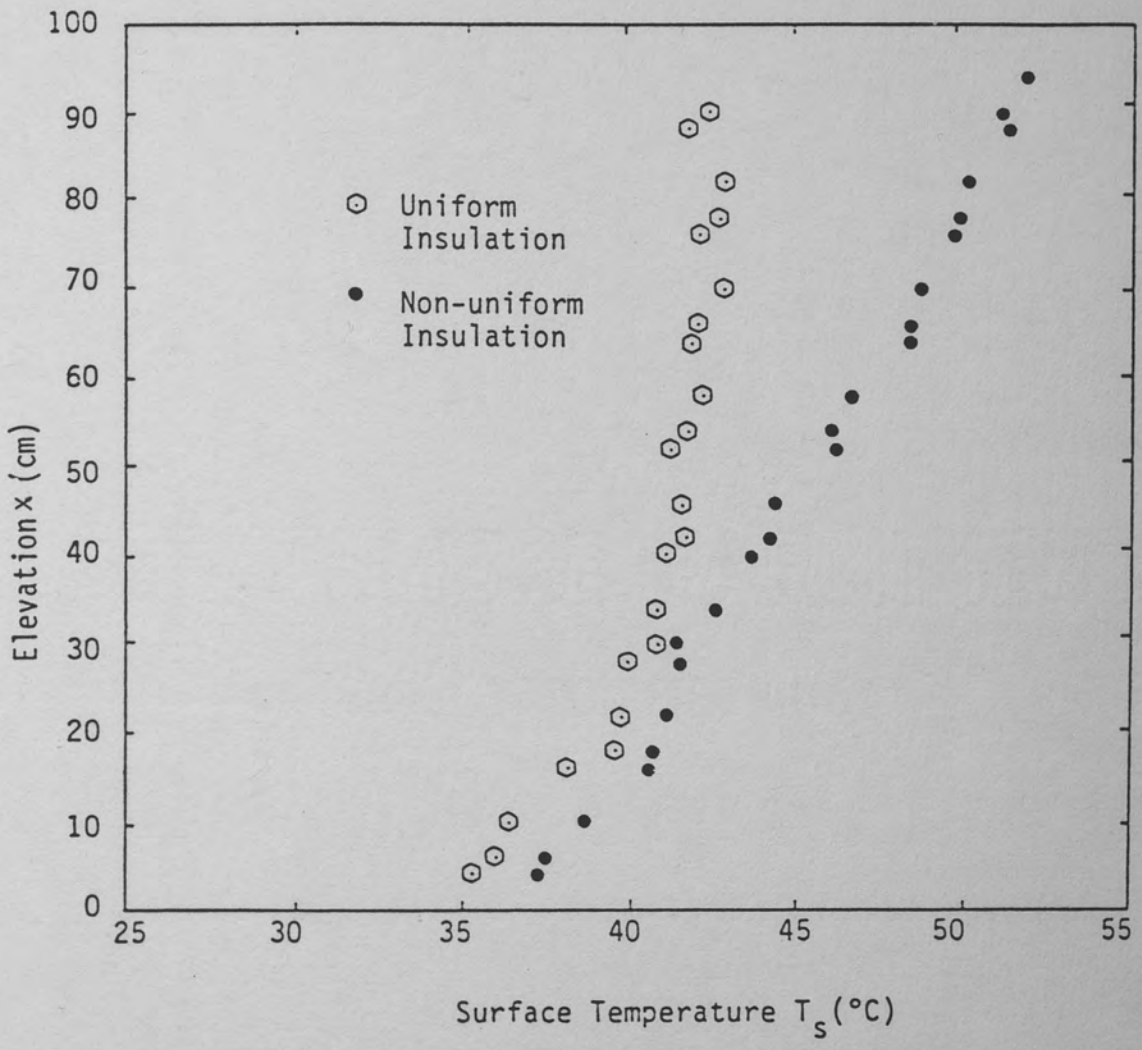

Figure 3.3. Axial surface temperature variation along the length of the tube.

TABLE 3.2
EXPERIMENTAL AND THEORETICAL [1] NUSSELT NUMBERS
AS A FUNCTION OF ELEVATION.

x (cm)	Nu (Exp)	Nu [1]	Discrepancies
3.5	6.53	12.5	48%
5.5	6.59		
9.5	6.45	8.2	21%
15.5	5.92		
17.5	6.00	7.0	14%
21.5	6.14		
27.5	6.58	6.5	1%
29.5	6.78		
33.5	6.55	6.0	9%
39.5	6.53		
41.5	6.36	5.8	10%
45.5	6.68		
51.5	6.26	5.5	14%
53.5	6.54		
57.5	6.42	5.3	21%
63.5	6.24		
65.5	6.32		
69.5	6.55	4.9	34%
75.5	6.58		
77.5	6.64		
81.5	6.83		
87.5	6.93	4.7	47%
89.5	7.14		
93.5	7.25	4.7	54%

L = 975 mm
D = 14.3 mm
q" = 140 Watts per square meter

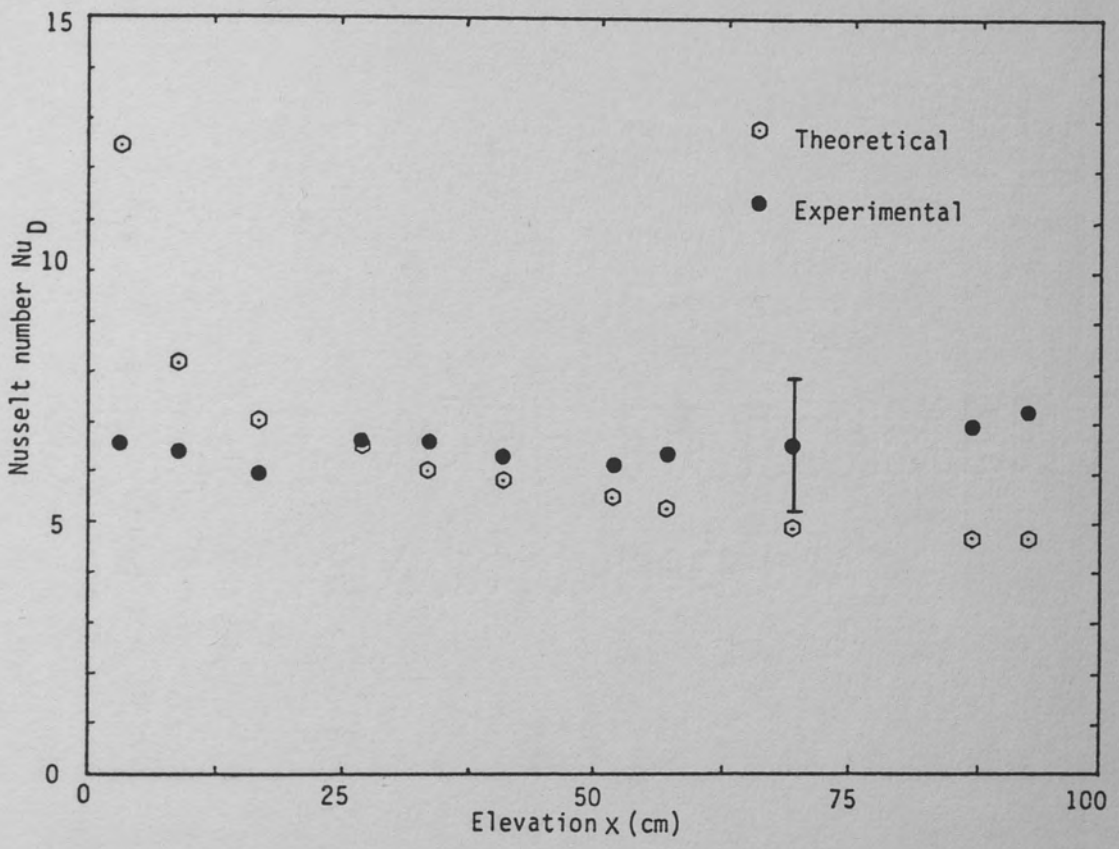

Figure 3.4. Nusselt number variation along the length of the tube.

3.4 Results and Discussion

In this section the results of this study are presented and compared with theoretical models.

As mentioned in Chapter 2, most studies involving thermal convection reduce to an evaluation of heat transfer coefficient or Nusselt number and its dependence on the boundary conditions. The details of evaluating the above quantities are presented in Appendix C. The experimental and theoretical [1] Nusselt numbers were given in Table 3.2 and illustrated in Figure 3.4, for a uniform tube heat flux. Results for a non-uniform heat flux are given in Appendix B.

As indicated in the previous section, the first step involved measuring surface temperature versus elevation of tube at a uniform heat flux. The effects of the entry region and the non-linear behavior of the thermal boundary layer is evident up to an elevation of approximately 30 centimeters. The heat transfer coefficient in this region drops drastically from entrance to this point. A more predictable and linear behavior can be seen beyond an elevation of 30 centimeters. The surface temperature in this fully developed

region increases steadily and the decrease in heat transfer coefficient is slower in pace compared to entry region.

Of specific interest to this study involved evaluating the Nusselt number from the experimental results. A detailed procedure to evaluate this quantity is outlined in Appendix C. Table 3.2 and Figure 3.2 show the results. The results of a theoretical investigation by Davis and Perona [1] for a similar situation are also shown for comparison. Their study assumed a stable and laminar flow in a vertical tube heated with constant heat flux. The incompresible thermal boundary layer equations were solved by using the finite difference method and they calculated velocity and temperature distributions throughout the tube. Additionally, they assumed the fluid enters at ambient temperature and with a flat velocity profile.

The variation of Nusselt number for the current study and the theoretical work of Davis and Perona [1] are illustrated on Figure 3.2.

The discrepences in the Nusselt number compared with the theoretical work of Davis and Perona [1] can be attributed to several related phenomena. The first difficulty encountered was maintenance of constant heat flux conditions with a usual resistance type heating technique. Several other factors influencing the test included irregular switching on/off conditions of the central air

conditioning system, the opening and closing of doors, the errors associated in the electrical measuring instruments and several other enviromental related problems affecting stability of natural convection type experiments.

As seen in Table 3.2, the range of errors is estimated to be 1 to 54 % in the fully developed region of the experiments, perhaps due to the above-mentioned difficulties.

An error analysis is performed for the experimental data which is given in Appendix E. This analysis suggest that the experimental Nusselt numbers may be in error to about ±25%, and if this error is taken into consideration the experimental results would compare favorably with the theoretical work of Davis and Perona [1]. However, the results achieved by Pasamehmetoglu [2] are in close agreement with the theoretical work of Davis and Perona [1].

4. Recommendations and Conclusions

From the experience gained through the subject experiments with natural convection, several suggestions are made.

i) Replace the electrical resistance heating method for maintaining a uniform heat flux on the tube. A more sophisticated heating technique involving infrared waves or other modes of energy dissipation may be necessary. The above arrangement would also facilitate variable heat flux conditions quite easily.

ii) Additional sensors (thermocouples) would be necessary for improving data collection and consequently the accuracy of the results.

iii) A very stable and quiet enviroment reflecting conditions suitable for natural convection is necessary.

iv) Experiments on different length and tube diameter would be necessary to fully understand the thermal mechanism, especially in the entrance region of the tube.

v) In order to substantiate the theoretical results in the entrance region, more sophisticated laser velocimeter

data for the velocities could be employed in evaluations of the Nusselt number.

vi) More experiments should be performed for a wide range of Grashof numbers to understand the behavior of the velocity and temperature profiles in both the entrance and the fully developed regions.

vii) Experiments with the above improvements would provide the necessary framework to provide a correlation for the Nusselt number valid in both entrance as well as fully developed region.

The results of this study suggest that discrepancies may remain between experiment and theory. When the propagation of potential experimental errors are considered, the experimental and theoretical free convection heat transfer behaviors have been shown to compare favorably. Further experimental efforts, incorporating the above recommendations, are suggested.

Appendix A

Theoretical Consideration

In this section the analytical solution to the problem being considered is solved by Pasamehmetoglu [2].

His solution is restricted to fully developed conditions. The fully developed conditions can be assumed to be reached when the hydrodynamic boundary layer thickness is approximately equal to the cylinder radius. The entry length was computed by using the approximate solution for the case of a flat plate,where

$$x_{entry} \cong R[\ Gr_R^* / ((1810/Pr)+(2260/Pr^2))] \qquad (A.1)$$

The expression is obtained by adapting the Von Karman approximate solution [14] to the problem of natural convection at constant heat flux for a vertical flat plate. The solution which follows is valid for $x > x_{entry}$.

The basic governing equations (continuity, momentum, and energy) are given by the following expressions:

$$(\partial u/\partial x) = 0 \qquad (A.2)$$

$$\nu[(1/r)\partial/\partial r(r\partial u/\partial r)]+R^2 g\beta(T-T_o)=0 \qquad (A.3)$$

$$\alpha[(1/r)\partial/\partial r(r\partial T/\partial r)]-R^2 u(\partial T/\partial x)=0 \qquad (A.4)$$

The solution technique are as follow;

The temperature is given by:

$$T(x,r)=T_o(x)+f(r) \qquad (A.5)$$

where T (x) is the centerline temperature and is a linear function of x; of the form:

$$T_x(x)= C_1 x+C_2 \qquad (A.6)$$

$$T_o(x)= C_1 x+C_2 \qquad (A.7)$$

Equations (A.2) through (A.7) are combined into a fourth order differential equation,

$$A[r^4(d^4u/dr^4)+2r^3(d^3u/dr^3)-r^2(d^2u/dr^2)+r(du/dr)]+r^4u=0 \qquad (A.8)$$

where A is a nondimensional constant,

$$A = \alpha\nu/g\beta C_1 R^4 \qquad (A.9)$$

Equation (A.8) is solved by using the Frobenius Method, and the following infinite series solutions were obtained for the velocity and temperature profiles; respectively:

$$u(r)= K_1 r^2 \sum_{n=0}^{\infty} ((-1)^n r^{4n})/(A^n[2^{2n}(2n+1)!]^2)+$$

$$+K_2 \sum_{n=0}^{\infty} ((-1)^n r^{4}n)/(A^n[2^{2n}(2n)!]^2) \qquad (A.10)$$

$$f(r)= -\nu/g\beta R^2[K_1 \sum_{n=1}^{\infty} ((-1)^n(4n+2)^2)(r^{4n})/(A^n(2^{2n}(2n+1)!)^2))$$

$$K_2 \sum_{n=1}^{\infty} ((-1)^n(4n)^2(r^{4n-2})/(A^n(2^{2n}(2n)!)))] \qquad (A.11)$$

where K_1 and K_2 are the integration constants determined by using the boundary conditions imposed on the velocity and the temperature.

Pasamehmetoglu assumed "A" to be 10^{-2}, the higher order terms in equations (A.10) and (A.11) can be neglected, and

the velocity and temperature profiles can be approximated as:

$$u(r) \cong K_1 r^2[1- (r^4/576A)]+K_2[1- (r^4/64A)] \qquad (A.12)$$

$$f(r) \cong \nu/g\beta R^2[K_1((r^4/16A)-(r^8/36864A^2))+K_2((r^2/4A)-(r^6/2304A^2))] \qquad (A.13)$$

The following boundary conditions are used to determine K_1 and K_2:

at $r=1$ $\qquad u(1)=0 \qquad (A.14a)$

$$(df/dr)= \dot{q}'_w/ 2\pi K \qquad (A.14b)$$

To determine the nondimensional constant A, Pasamehmetoglu used the conservation of energy principle:

$$\dot{q}'_w = \dot{m} C_p (\partial T/\partial x) \qquad (A.15)$$

where

$$\dot{m} = R^2 \int_0^1 \rho u(r) 2\pi r dr \qquad (A.16)$$

and

$$(\partial T/\partial x) = (dT_o/dx) = C_1 \qquad (A.17)$$

Both $\dot{m}$ and C_1 can be written in terms of A. Substituting (A.16) and (A.17) into (A.15) and solving the resulting equation yields $A=1.16(10)^{-2}$ which is in agreement with Pasamehmetoglu original assumption.

From this analysis, Pasamehmetoglu provides the resulting velocity and temperature profiles as follow:

$$u(r) = \frac{1}{2\pi} \cdot \frac{\nu}{R} \cdot Gr_R^* \cdot 10^{-2}(3.14 + 1.28r^2 - 4.23r^4 - 0.19r^6) \qquad (A.18)$$

$$f(r) = \frac{1}{2\pi} \cdot \frac{\dot{q}_w'}{K} \cdot 10^{-2}(67.67r^2 + 6.9r^4 - 10.13r^6 - 0.26r^8) \qquad (A.19)$$

Plots of Equations (A.18) and (A.19) are shown in Figures (A.1) and (A.2), respectively.

The mass flow rate and the heat transfer correlations can be computed, since the velocity and temperature profiles are now known.

The mass flow rate is found by using Equation (A.18) and the result can be nondimensionalized to yield:

$$Re_R = 1.16(10)^{-2}\ Gr_R^* \qquad (A.20)$$

The heat transfer coefficient is given by:

$$h = \dot{q}_w' /((T_w-T_b)2\pi R \qquad (A.21)$$

where

$$T_b =([\int_0^1 f(r)u(r)rdr]/[\int_0^1 u(r)rdr])+T_o(x) \qquad (A.22)$$

Using Equations (A.18) and (A.19), the following results are obtained:

$$T_b = (0.212\ \dot{q}_w' /2\pi K)+T_o(x) \qquad (A.23)$$

$$T_w = (0.642\ \dot{q}_w' /2\pi K)+T_o(x) \qquad (A.24)$$

Finally, the heat transfer coefficient can be expressed in nondimensional form, to yield a constant given by:

$$Nu = 2.326$$

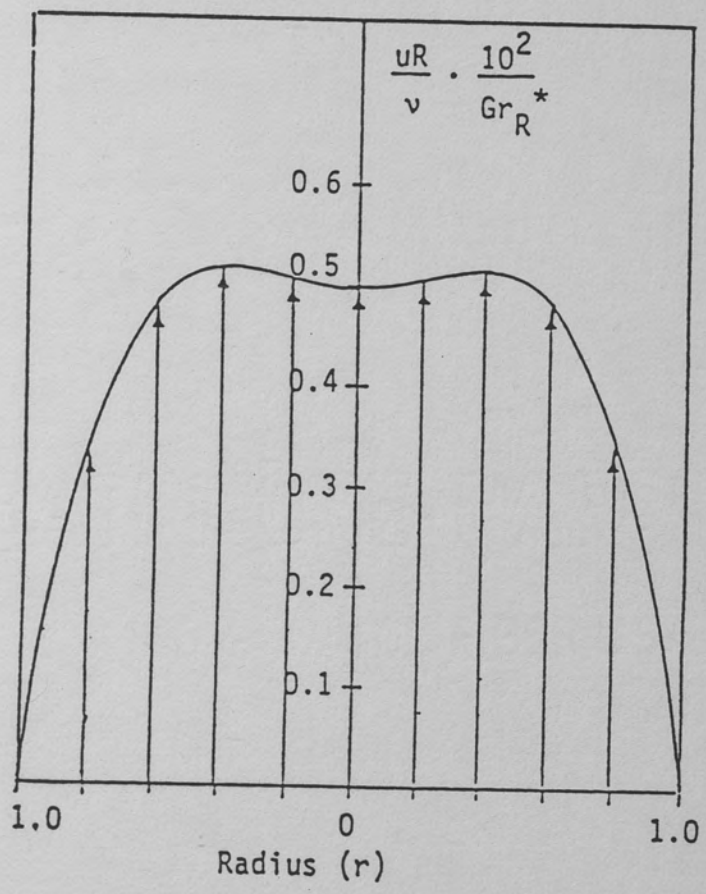

Figure A.1. Fully developed velocity profile. Reference [2].

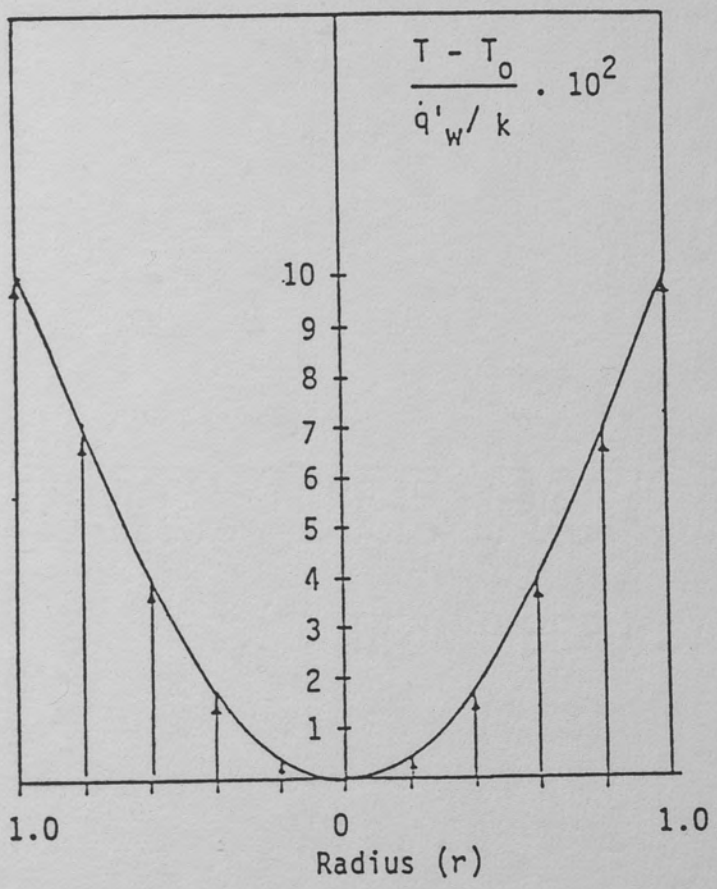

Figure A.2. Fully developed temperature profile. Reference [2].

Appendix B

Experimental Data

It was mentioned in the experimental section that a non-uniform insulation thickness was required to maintain a constant heat flux. An analysis of the external free convection around the insulation, and conduction through the insulation is discussed below.

The insulation outer surface temperatures measured along the length of the tube for uniform and non-uniform thermal insulation are presented in Table B.1 and in Figure B.1.

The test section incorporates eight interconnectable subsections. Call the upstream subsection "one" and the down stream subsection "eight". The heat loss analysis follows.

Outer surface uniform insulation temperature measurements were taken for the eight subsections, and the data are presented in Table B.2 along with the heat losses by free convection to the atmosphere surrounding the insulation. The convection heat transfer coefficient for the ambient air was to be five watts per square meter per degree

TABLE B.1
THE OUTER SURFACE AXIAL TEMPERATURES FOR A UNIFORM AND NON-UNIFORM THERMAL INSULATION. V=3 VOLTS.

x(cm)	T(°C) Uniform Insulation	T(°C) Non-Uniform Insulation
3.5	35.1	37.2
5.5	35.8	37.4
9.5	36.2	38.5
15.5	37.9	40.5
17.5	39.4	40.6
21.5	39.5	41.0
27.5	39.7	41.4
29.5	40.6	41.3
33.5	40.6	42.4
39.5	40.9	43.5
41.5	41.5	44.1
45.5	41.3	44.2
51.5	41.0	46.1
53.5	41.5	45.9
57.5	41.9	46.6
63.5	41.7	48.3
65.5	41.8	48.4
69.5	42.6	48.7
75.5	41.9	49.6
77.5	42.4	49.8
81.5	42.6	50.1
87.5	41.5	51.2
89.5	42.1	51.1
93.5	41.7	51.8

L = 975 mm
D = 14.3 mm

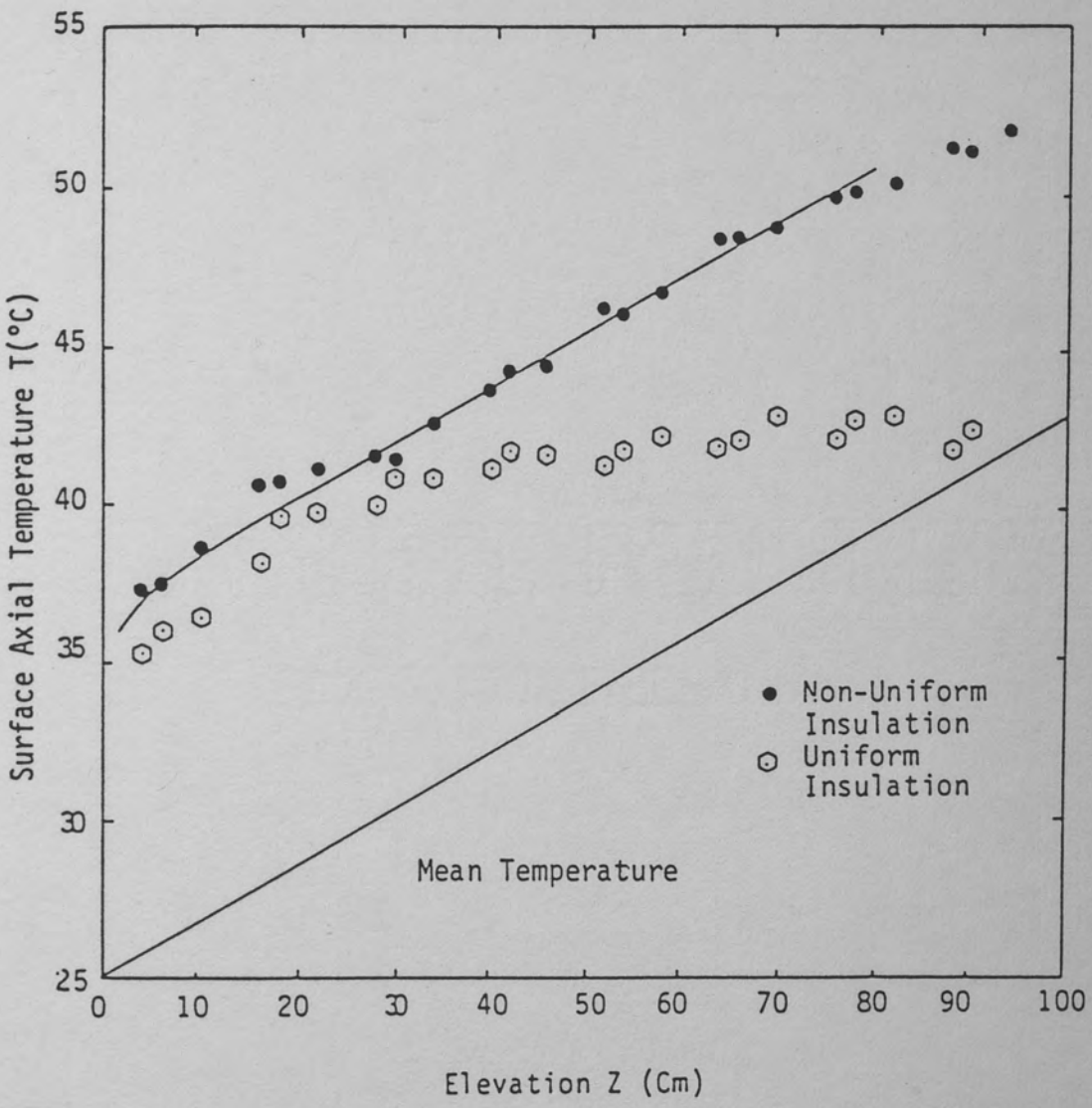

Figure B.1. Axial surface temperature variation along the length of the tube for uniform and non-uniform thermal insulation.

Kelvin. A sample calculation for subsection " one" follows:

Governing equation:

$q'' = h (T_s - T_\infty)$

where,

$T_s = 27.1$ ℃

$T_\infty = 25.0$ ℃

$h = 5.0$ W/m^2-K (free convection, vertical cylinder)

Upon substitution:

$q'' = 10.5$ watts/square meter

The procedure for the other seven subsections are the same.

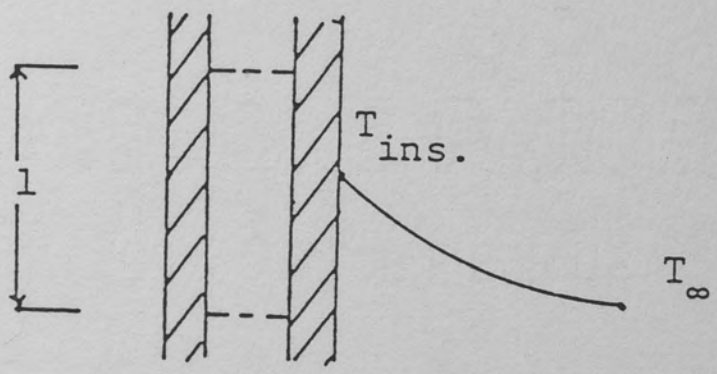

Figure B.2. Sketch of a section along the length of the tube.

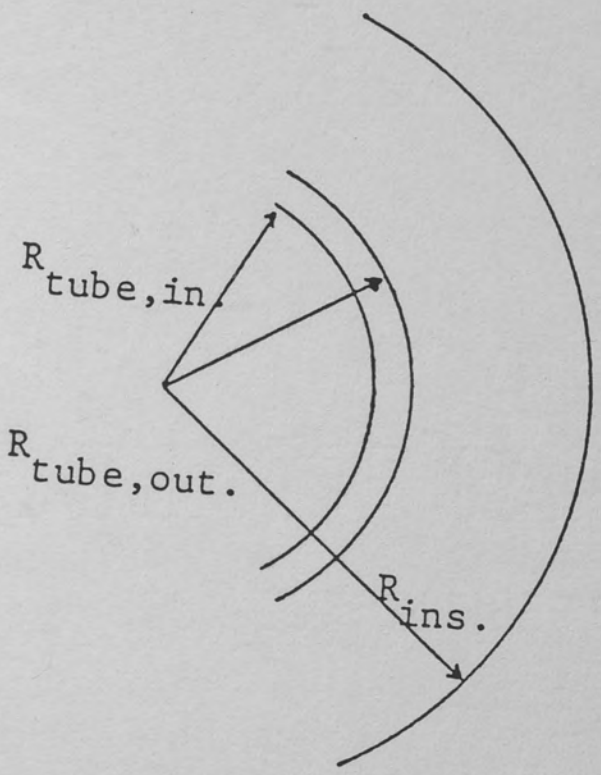

Figure B.3. Top view of the tube.

Table B.2

OUTER SURFACE TEMPERATURE OF THE UNIFORM INSULATION

Subsection	Outer Surface temp. of the Ins. (℃)	External Heat loss by free Conv. (W/m^2-K)
1	27.1	10.5
2	27.3	11.5
3	27.4	12.0
4	27.6	13.0
5	27.7	13.5
6	28.3	17.5
7	28.6	18.0
8	28.8	19.0

Room temperature: 25.0 ±1.0°℃

L = 975 mm
D = 14.3 mm
q''_{net} = 140 Watts per square meter

The experiment was also performed at other power levels (3, 12.1,18.9 watts) with a uniform thermal insulation. The axial outer surface temperature measurements are presented in Table B.3.

A non-uniform thermal insulation was considered necessary to better maintain a uniform heat flux. Insulation outer surface temperature measurements were taken for the eight subsections, and they are presented in Table B.4 along with the respective heat losses. The calculation was the same as for the uniform insulation case.

$$q = 10.0 \text{ watts/Square meter}$$

Consideration of heat losses from the uniform and non-uniform thermal insulation were presented in Table B.2 and Table B.4, respectively. One can easily see that a non-uniform thermal insulation gives a better uniform heat flux, and this could be seen from Figure B.4 which provides the net heat flux for the uniform and non-uniform thermal insulation, and this was one of the first design objectives of this study.

TABLE B.3
THE AXIAL SURFACE TEMPERATURES FOR A UNIFORM THERMAL INSULATION OF THREE OTHER POWER INPUTS

x(Cm)	3.0 watts T (°C)	12.1 watts T (°C)	18.9 watts T (°C)
3.5	30.2	43.1	50.0
5.5	30.7	44.6	52.1
9.5	30.9	45.0	52.6
15.5	31.5	46.3	54.5
17.5	32.4	47.6	56.2
21.5	32.4	46.7	53.6
27.5	32.6	46.4	55.6
29.5	33.2	46.5	55.4
33.5	33.0	46.3	55.7
39.5	32.7	51.4	62.0
41.5	33.4	51.3	61.9
45.5	33.2	51.5	61.7
51.5	32.7	50.8	60.9
53.5	32.8	51.9	62.3
57.5	33.2	52.9	63.9
63.5	33.4	51.7	61.3
65.5	33.6	52.4	62.3
69.5	33.9	53.3	63.3
75.5	33.5	52.6	63.4
77.5	33.7	54.3	67.7
81.5	33.8	54.0	66.7
87.5	32.7	53.5	66.1
89.5	33.0	55.7	66.4
93.5	33.3	54.6	66.9
T,out	32.3	47.4	60.5

Room temperature: 25± 1 °C
L = 975 mm
D = 14.3 mm

TABLE B.4
OUTER SURFACE TEMPERATURE OF THE NON-UNIFORM INSULATION

Subsection	Insulation temp.(°C)	Heat loss (watts)/m^2
1	27.0	10.0
2	27.5	12.5
3	27.3	11.5
4	27.5	12.5
5	27.6	13.0
6	27.8	14.0
7	27.5	12.5
8	27.3	11.5

L = 975 mm
D = 14.3 mm
q" = 140 Watts per square meter
Room temperature: 25 ±1 °C

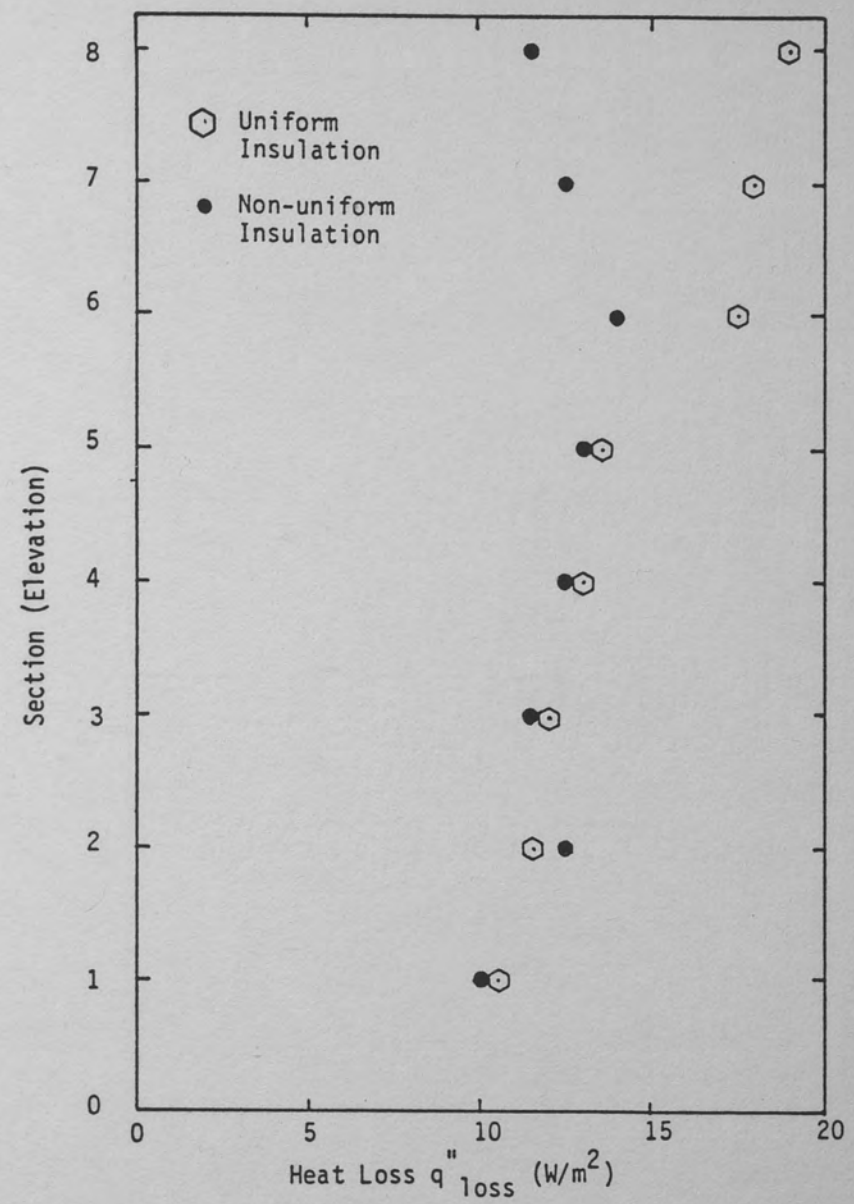

Figure B.4. Variation of heat loss for uniform and non-uniform thermal insulation.

APPENDIX C

Sample Calculations

The amount of heat which was generated by the power supply is:

$$q = V^2/R \qquad (C.1)$$

where "V" is the voltage, and "R" is the resistance of the copper wire (AWG of size 20).

V = 3 volts

R = 1.32 Ohms

Upon substitution;

q = 6.82 watts

As shown in Appendix B, there is some heat loss through the insulation and Table B.4 shows the approximate heat loss of 12 watts per square meter. Then the net heat flux on the surface of the tube follows:

$$q'' = (q / A_s) - 12 \qquad (C.2)$$

where q = 6.82 watts, and A_s = Surface area = π D L

where D = 0.0143 m, and L = 0.975 m

Upon substitution;

q" = 141 watts/square meter

The mass flow rate is calculated by the following equation,

$$q'' = \dot{m} C_p (T_{out} - T_{in}) \qquad (C.3)$$

where , typically,

q" = 6.17 watts

C_p = 1017 J/Kg- K

T_{in} = 25 °C

T_{out} = 42.9 °C

Upon substitution;

$\dot{m}$ = 3.38(E-4) Kg/s

To experimentally find the local Nusselt number along the tube, a sample calculation is shown below for an elevation of 3.5 centimeters.

$q'' = h (T_s - T_m)$ (C.4)

$Nu_D = h D/K$ (C.5)

where q'' = 141 watts/Square meter

T_s = Axial surface temperature of the tube (at z = 3.5 centimeter) = 37.2 °C.

T_m = Mean temperature (at z = 3.5 centimeters) = 25.6 °C. (The value of T_m is read from Figure B.1).

Combining Equations (C.4) and (C.5);

$Nu_D = (q''_{net} .D)/[K (T_s - T_m)]$

Upon substitution;

$Nu = 6.53$

The Reynolds number is calculated as follows:

$Re_D = 4 \dot{m} / \pi D\mu$ (C.6)

where,

$m = 3.38$ (E-4) Kg/s

$D = 0.0143$ m

(Dynamic viscosity) = 184.6 (E-7) N-s/m

Upon substitution;

$Re_D = 1631$

To find the Nusselt number theoretically [1], one has to perform the following procedure,

$$Gr_I^* = [g(q''_{net})\ R^5]/[\ \bar{T}_o L\nu^2 K] \qquad (C.7)$$

where,

$(q/A)_{net}$= 141 W/square meter

R (radius of the tube) = 0.0072 m

$\bar{T}_o$ (Absolute ambient air temperature) = 298 K

L = 0.975m

ν (Kinematic viscosity) = 15.89 (E-6) m/s

K (Thermal conductivity of air)= 26.3 (E-3) W/m.K

Upon substitution;

Gr_I^* = 13.86

Then the dimensionless tube length "L " is defined by [1]:

$$L' = L/Gr^* = 0.072 \qquad (C.8)$$

From Figure(C.1) the dimensionless volumetric flow rate can be read as:

F (Dimensionless volumetric flow rate) = 0.085

Now one has to find the following dimensionless parameter for each axial position, illustrated in Table (C.1). For example;

$Z/Re\ Pr\ D = 2\ (10)^{-3}$ at $Z = 3.5$ cm.

At this stage the local Nusselt number [1] can be read from Figure (C.2).

TABLE C.1

THEORETICAL NUSSELT NUMBER AT DIFFERENT ELEVATIONS
ACCORDING TO DAVIS AND PERONA [1]

x (Cm)	$\{Z/Re\ Pr\ D\}(10)^{-2}$	Nu [1]
3.5	0.2	12.5
5.5	0.3	
9.5	0.6	8.2
15.5	0.9	
17.5	1.0	7.0
21.5	1.3	
27.5	1.6	6.5
29.5	1.7	
33.5	1.9	6.0
39.5	2.3	
41.5	2.4	5.8
45.5	2.6	
51.5	3.0	5.5
53.5	3.1	
57.5	3.3	5.3
63.5	3.7	
65.5	3.8	
69.5	4.0	4.9
75.5	4.3	
77.5	4.5	
81.5	4.7	
87.5	5.0	4.7
89.5	5.1	
93.5	5.4	4.6

L = 975 mm
D = 14.3 mm
q" = 140 Watts per square meter

TABLE C.2

VARIATION OF THE MEAN TEMPERATURE AND THERMAL CONDUCTIVITY ALONG THE LENGTH OF THE TUBE

x (Cm)	T (°C)	T (°C)	K (W/m-K)
3.5	25.6	37.2	26.6
5.5	25.9	37.4	26.6
9.5	26.8	38.5	26.7
15.5	27.8	40.5	26.8
17.5	28.1	40.6	26.8
21.5	28.8	41.0	26.9
27.5	30.0	41.4	26.9
29.5	30.3	41.3	27.0
33.5	31.0	42.4	27.0
39.5	32.1	43.5	27.1
41.5	32.4	44.1	27.1
45.5	33.1	44.2	27.2
51.5	34.3	46.1	27.3
53.5	34.6	45.9	27.3
57.5	35.1	46.6	27.3
63.5	36.5	48.3	27.4
65.5	36.8	48.4	27.5
69.5	37.5	48.7	27.5
75.5	38.5	49.6	27.6
77.5	38.8	49.8	27.6
81.5	39.4	50.1	27.6
87.5	40.7	51.2	27.7
89.5	40.9	51.1	27.7
93.5	41.8	51.8	27.8

L = 975 mm
D = 14.3 mm
q" = 140 Watts per square meter

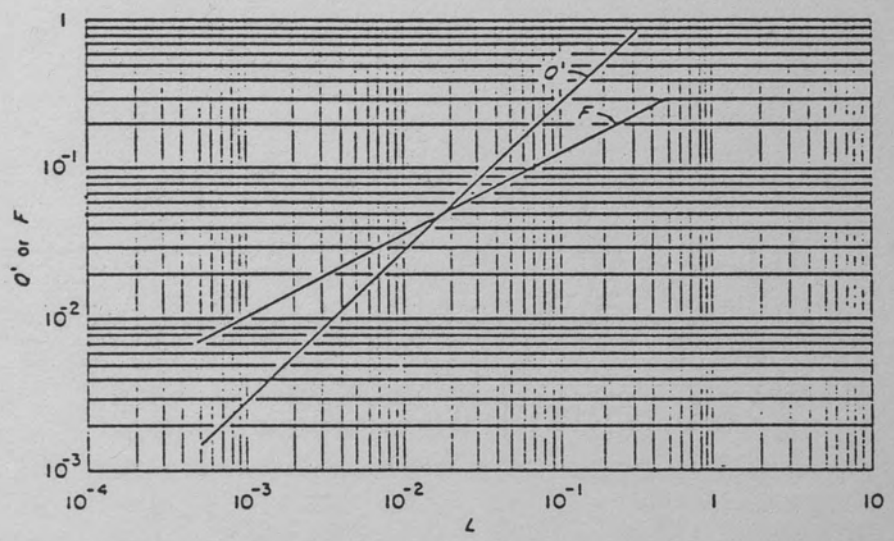

Figure C.1. Variation of dimensionless flow and heat absorbed with dimensionless tube length, constant wall heat flux, Reference [1].

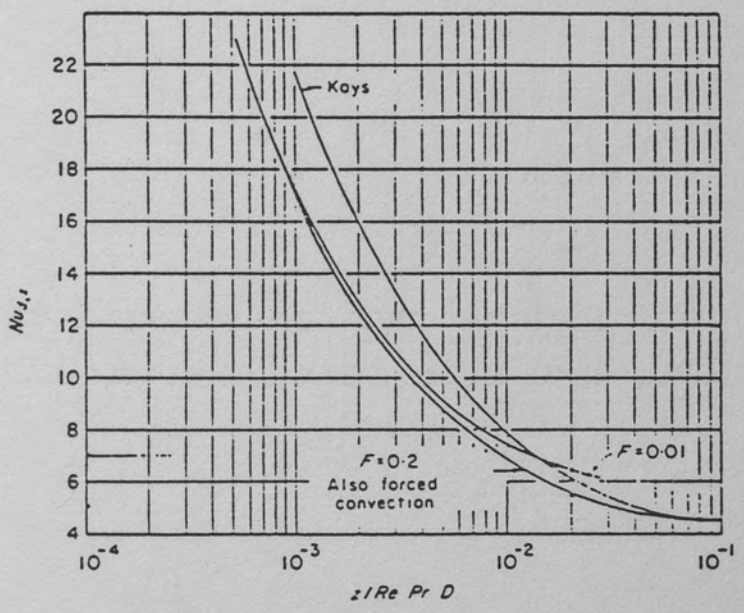

Figure C.2. Comparison of local Nusselt number with work of Kays, constant wall heat flux, Reference [1].

Appendix D

Physical properties

Properties of air at 300 K

Dynamic viscosity= 184.6E-7N-s/m

Kinematic viscosity= 15.89E-6 m /s

Thermal conductivity= 26.3E-3 W/m-K

Prandtl number= 0.707

Test conditions (typical)

Dry bulb temperature= 25.0°C

Wet bulb temperature= 20.0°C

Humidity ratio, ω, mass of water per mass of dry air = 88 grains per lb of dry air (psychometric chart)

C_p= 1017 J/Kg-K (0.2429 Btu/ F-lb of moist air),

Figure D.1

Heat transfer coefficient on the outer insulation surface = 5.0 W/m^2-K. (assumed)

Properties of Insulation

Thermal conductivity of the insulation= 0.035 W/m-K

Properties of Copper tube

(Properties at 300 K)

Thermal conductivity = 403 W/m-K

Density = 8933 Kg/cubic meter

Specific Heat = 376.5 J/Kg-K

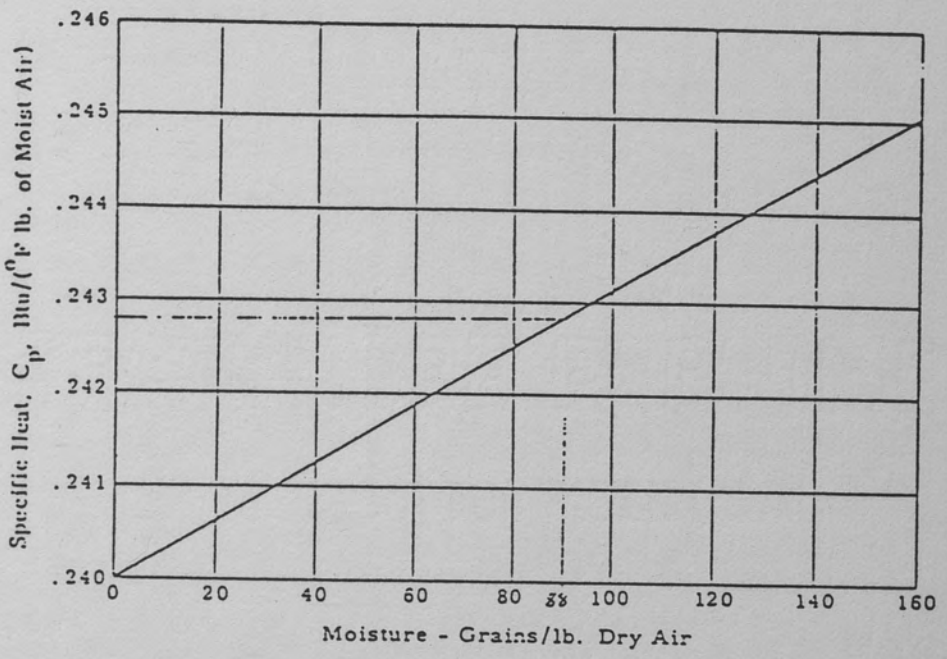

Figure D.1. Effect of humidity on the specific heat of air, Reference [15].

Appendix E

Uncertainty Analysis

The purpose of this section is to provide the uncertainty analysis of the data gathered. In order to do such an analysis a method of estimating uncertainty in experimental results has been presented by Kline and McClintok [16]. They provided an implicit relationship which follows:

$$w_R = [((\partial R/\partial x_1)(w_1))^2 + ((\partial R/\partial x_2)(w_2))^2 + \ldots + ((\partial R/\partial x_n)(w_n))^2]^{\frac{1}{2}} \quad (E.1)$$

where w_R is the uncertainty in the results and w_1, w_2, ..., w_n is the uncertainty in the independent variables.

The above method is used to yield the following results.

$$Nu_D = f(q'', D, Ts, Tm, K) \quad (E.2)$$

$$\partial Nu/\partial q'' = D/(T_s - T_m) K \quad (E.3a)$$

$$\partial Nu/\partial D = q''/(T_s - T_m) K \quad (E.3b)$$

$$\partial Nu/\partial T_s = -(q''D)/K(T_s - T_m)^2 \quad (E.3c)$$

$$\partial Nu/\partial T_m = (q''D)/(T_s - T_m) K^2 \quad (E.3d)$$

(E.3e)

where, at x = 93.5 cm.

$q'' = 141\ w/m^2 \pm 10\%$

$D = 0.0143\ m \pm 0.001m$

$K = 27.8(10) \pm w/m\text{-}k\ \ 1\%$

$T_s = 51.8\ ^\circ C \pm 1\ ^\circ C$

$T_m = 41.8\ ^\circ C \pm 1\ ^\circ C$

Upon substitution into Equations (E.3a) through (E.3e);

$\partial Nu/\partial q'' = 0.051$

$\partial Nu/\partial D = 507.2$

$\partial Nu/\partial T_s = -0.73$

$\partial Nu/\partial T_m = 0.73$

$\partial Nu/\partial K = -261$

Then;

$w_{q''} = (141)(0.1) = 14.1\ w/m^2$

$w_D = 0.001m$

$w_{T_s} = 1°C$

$w_{T_m} = 1°C$

$w_K = (27.8(10)^{-3})(0.01) = 27.8(10)^{-5}\ w/m\text{-}k$

Thus, the uncertainty in the Nusselt number is;

$$w_{Nu_D} = 1.36 \text{ or } 18.7\%$$

REFERENCES

1. Davis, L.P., and Perona, J.J. "Development of Free Convection Flow of a Gas in a Heated Vertical Open Tube." International Journal of Heat and Mass Transfer 14 (July 1970): 889-903.

2. Private Communications with Pasamehmetoglu,K. University of Central Florida. Orlando, Florida. April 1986.

3. Incorpera, F.P., and Dewitt, D.P. Fundamentals of Heat Transfer. New York: John Wiley & Sons, 1981.

4. Iderriah, F.J.K. "An International Relaxation Method of Curing Numerical Instability in Prediction of Flows Influenced by Severe Body Forces." Journal of Mechanical Engineering Sciences. 22 (June 1980): 153-156.

5. Elenbaas, W. "Heat Dissipation of Parallel Plates by Free Convection." Physica 9 (September 1942): 865-874.

6. Bodoia, J.R., and Osterle, J.F. "The Development of Free Convection Between Heated Vertical Plates." ASME Journal of Heat Transfer 84, (February 1962): 40-44.

7. Aung, W. "Fully Developed Laminar Free Convection Between Vertical Plates Heat Asymmeytrically." International Journal of Heat and Mass Transfer 15 (September 1972): 1577-1580.

8. Miyatake, O., and Fujii, T. "Free Convective Heat Transfer Between Vertical Parallel Plates - One Plate Isothermally Heated and the Other Thermally Insulated." Heat Transfer Japanese Research 3 (1972): 30-38.

9. Sparrow, E.M., and Gregg, J.L. "Laminar Free Convection from a Vertical Plate with Uniform Surface Heat Flux." Transactions of American Society of Mechanical Engineers 78 (February 1956): 435.

10. Miyatake, O., Fujii, T., Fujii, M., and Tanaka, H. "Natural Convection Heat Transfer Between Vertical Parallel Plates - One Plate with a Uniform Heat Flux and the Other Thermally Insulated." Heat Transfer Japanese Research 4 (1973): 25-33.

11. Wirtz, R.A., and Stutzman, R.J. "Experiments on Free Convection Between Vertical Plates with Symmetric Heating." Journal of Heat Transfer 104 (August 1982): 501-507.

12. Aung, W., Fletcher, L.S., and Sernas, V. "Developing Laminar Free Convection Between Vertical Plates and Asymmetric Heating." International Journal of Heat and Mass Transfer 15 (February 1972): 2293-2308.

13. Kays, W.H. "Numerical Solution for Laminar Flow Heat Transfer in Circular Tubes." Transactions of American Society of Mechanical Engineers 71 (November 1955): 1265.

14. Holman, J.P. Heat Transfer. New York: McGraw Hill, 1976.

15. General Electric. General Electric Notes, Section 504.1. Daytona Beach, Florida: General Electric, 1984.

16. Holman, J.P. Experimental methods for Engineers. New York: McGraw Hill, 1984.